Optics Letters

Quantitative spectroscopy of single molecule interaction times: supplement

H.-H. BOLTZ,[1,2,5] A. SIRBU,[2] N. STELZER,[2] M. J. LOHSE,[2,3] C. SCHÜTTE,[1,4] AND P. ANNIBALE[2,6]

[1]*Zuse Institute Berlin (ZIB), 14195 Berlin, Germany*
[2]*Max Delbrück Center for Molecular Medicine, 13125 Berlin, Germany*
[3]*University of Würzburg, Institute of Pharmacology and Toxicology, 97078 Würzburg, Germany*
[4]*Freie Universität Berlin, Institut für Mathematik, 14195 Berlin, Germany*
[5]*e-mail: boltz@zib.de*
[6]*e-mail: paolo.annibale@mdc-berlin.de*

Supplemental Document to "Quantitative spectroscopy of single molecule interaction times"

H-H. BOLTZ,[1,2,*] A. SIRBU,[2] N. STELZER,[2] M. J. LOHSE,[2,3] C. SCHÜTTE,[1,4] AND P. ANNIBALE[2,*]

[1]*Zuse Institute Berlin (ZIB)*
[2]*Max Delbrück Center for Molecular Medicine, Berlin*
[3]*University of Würzburg, Institute of Pharmacology and Toxicology*
[4]*Freie Universität Berlin, Institut für Mathematik*
[*]*Corresponding authors: boltz@zib.de,paolo.annibale@mdc-berlin.de*

1. First-passage times

At time $t = 0$ a point particle subject to Brownian motion enters a radially symmetric (circular/spherical) region of interest (ROI) with radius R; we want to determine the distribution P_l of times it lingers within this region, which is the distribution of first-passage time of the distance r of the particle to the center of the ROI.

The Brownian motion is characterized by its Fokker-Planck equation, the diffusion equation,

$$\partial_t \Phi(\boldsymbol{r}, t) = D\Delta\Phi(\boldsymbol{r}, t)$$

introducing the diffusion constant D.

From dimensional analysis, it is obvious that the relevant timescale will be of the form

$$\tau \sim R^2/D$$

with a corresponding exponential cut-off to the distribution of the lingering times

$$-\log P_l^{R,D}(t) \sim t/\tau \qquad \text{for } t \gg \tau.$$

On shorter time-scales, the picture is different. Particles that only linger for a short time effectively do not explore the geometry, eliminating the R-scale and making the problem scale-free which would suggest a power-law dependence in P_l. Effectively the problem on this time-scale is one-dimensional (the distance to the border) and, thus, we expect to find the one-dimensional return exponent $\chi = 3/2$ and, therefore,

$$P_l^{R,D}(t) \sim t^{-3/2} \qquad \text{for } t \ll \tau.$$

Due the peculiar notion of the problem with the particle being initially right on the edge of the ROI, special attention is needed to $P_l(t = 0)$. Geometrically it is obvious that there is a singular part $P_l(t) \sim 1/2\delta(t)$ as half of all possibilities for the first motion of a particle right on the edge will lead to the particle not being within the ROI.

To determine the distribution of first-passage times through $r = R$ of a particle that is initially at $r = R - \varepsilon$ ($\varepsilon > 0$), i.e. we are looking for a Green's function $G(\boldsymbol{r}, t)$ to the diffusion equation with the boundary condition $G(\boldsymbol{r}, t)|_{r=R} = 0$ and the initial condition $G(\boldsymbol{r}, 0) \propto \delta(\boldsymbol{r} - \boldsymbol{r}_0)$ with $r_0 = |\boldsymbol{r}_0| = R - \varepsilon$. From this the distribution of passages through the boundary can then be determined from the flux through it

$$P_l^\varepsilon(t) = \int_{|\boldsymbol{r}|=R} D\partial_r G(\boldsymbol{r}, t).$$

The approach to determining G is independent of the dimension we use a bilinear decomposition $G(\boldsymbol{r}, t) = \sum_n \exp \lambda_n t \psi_n(\boldsymbol{r}) \psi_n(\boldsymbol{r}_0)$ where ψ_n are the eigenfunctions corresponding to

$$\lambda_n \partial_t \psi_n = D \Delta \psi_n$$

with the stated boundary conditions.

Three dimensions In three dimensions, the radial part of the Laplacian is $\Delta_r \psi_n = \frac{1}{r} \partial_r^2 (r\psi)$ from which we see that a suitable set of solutions is given by $\psi_n = r^{-1} \sin n\pi r / R$ with $\lambda_n = -D(n\pi/R)^2$. Thus, we find

$$G(\boldsymbol{r}, t) \propto \sum_{n=1}^{\infty} \frac{\sin \frac{n\pi r}{R}}{r} \frac{\sin \frac{n\pi r_0}{R}}{r_0} e^{-D(n\pi/R)^2 t}$$

and

$$P_l^\varepsilon(t) \propto \sum_{n=1}^{\infty} n \sin \frac{n\pi\varepsilon}{R} e^{-D(\pi n/R)^2 t}.$$

From this, we can read the dominant timescale, $\tau_1 = R^2/(\pi^2 D) \approx 1/(9.87) R^2 / D$.

Two dimensions In two dimensions, things are similar. We have to replace the sine by the zeroth Bessel function J_0 (with $J_1 = -J_0'$ denoting the first Bessel function) of the first kind and whose zeroes α_n determine the relevant modes, yielding

$$G(\boldsymbol{r}, t) \propto \sum_{n=1}^{\infty} J_0(\frac{\alpha_n r}{R}) J_0(\frac{\alpha_n r_0}{R}) e^{-D(\alpha_n/R)^2 t}$$

and

$$P_l^\varepsilon(t) \propto \sum_{n=1}^{\infty} -\alpha_n J_1(\alpha_n) J_0(\alpha_n r_0/R) e^{-D(\alpha_n/R)^2 t}.$$

There is ample room for simplification, but the important part is that the dominant (longest) timescale is given by $\tau_1 = R^2/(\alpha_1^2 D) \approx 1/5.78 R^2 / D$.

For a more general walk with $\Delta x^2 \sim \Delta t^{2\mu}$ ($\mu = 1/2$ being the standard Brownian case), a full analytical treatment might not be possible, but we can easily extend the intuitive arguments, by noting that the general return exponent would then be $\chi = 1 + \mu$. Thus, a careful analysis of the initial behaviour of the overlap time distribution (if available due to time resolution) can provide insight into the (short-time) dynamics.

Finally, we note that the initial $t^{-3/2}$ behaviour [1] for standard Brownian motion is indeed independent of dimension and also observed in blinking dot experiments [2]. This comes from the fact that the very fast trajectories effectively only explore one dimension (away from the boundary and back). However, the region of times on which this will be observable is dimensionally dependent (the algebraic part being shorter in higher dimensions).

2. Estimation of effective timescale

We are interested in the typical colocalization time of two particles that experience an attractive, binding interaction that is characterized by microscopic rates k_{on}, k_{off} and a range that is small compared to the colocalization region. We can make some ground by considering a very rough

description of the system formed by one pair by means of four states with Markovian transitions [3]: 1) A, the pair distance is within the colocalization region, but outside the interaction range; 2) B, the pair distance is within the interaction range, but the pair is not bound; 3) B′, the pair is bound; 4) C, the pair distance is outside the colocalization region. For the overlap time distribution, we are interested in the typical timescale the system takes from state A to state C. We describe the dynamics by introducing rates $k_{\text{off}}, k_{\text{on}}, k_{AB}, k_{BA}, k_{AC}$ that control the transitions

$$\text{B}' \underset{k_{\text{off}}}{\overset{k_{\text{on}}}{\rightleftharpoons}} \text{B} \underset{k_{BA}}{\overset{k_{AB}}{\rightleftharpoons}} \text{A} \overset{k_{AC}}{\longrightarrow} \text{C}. \tag{1}$$

To keep things simple, we first consider only the subsystem formed by

$$\text{B}' \underset{k_{\text{off}}}{\overset{k_{\text{on}}}{\rightleftharpoons}} \text{B} \overset{k_{BA}}{\longrightarrow} \text{A}$$
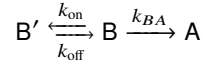
and ask for the time it takes from state B to A for the first time. Generally, speaking this will consist of cycles B, B′, B followed by single transition to A. The probability to transition from B to B′ is given by

$$P_{BB'} = \int_0^\infty \mathrm{d}t_1 \, k_{\text{on}} e^{-k_{\text{on}} t_1} \int_{t_1}^\infty \mathrm{d}t_2 \, k_{BA} e^{-k_2 t_2}.$$

This is a mere reflection of the logic that is at play in the Gillespie algorithm: both possible transitions have exponentially distributed transition times and the one with the smaller time actually happens. Of course, this is readily evaluated to

$$P_{BB'} = \frac{k_{\text{on}}}{k_{\text{on}} + k_{BA}},$$

from which we also directly gather that the expected number of trials for the first occurrence of A is

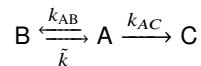$$n = \frac{k_{\text{on}} + k_{BA}}{k_{BA}}.$$

The average time spent on this is given by

$$\tau_{BA} = \frac{n}{k_{\text{on}} + k_{BA}} + \frac{n-1}{k_{\text{off}}} = \frac{1}{k_{BA}} + \frac{k_{\text{on}}}{k_{\text{off}} k_{BA}}$$

which corresponds to an effective rate

$$\tilde{k}_{BA} = \frac{1}{k_{BA}^{-1} + \frac{k_{\text{on}}}{k_{\text{off}} k_{BA}}}.$$

We can now address the effective rate k_{eff} for the transition between A and C by doing the same steps mutatis mutandis for the system

$$\text{B} \underset{\tilde{k}}{\overset{k_{AB}}{\rightleftharpoons}} \text{A} \overset{k_{AC}}{\longrightarrow} \text{C}$$

and using $K = k_{\text{on}}/k_{\text{off}}$ to end up with

$$k_{\text{eff}} = \frac{1}{k_{AC}^{-1} + \frac{k_{AB}}{\tilde{k} k_{AC}}} = \frac{k_{AC}}{1 + \frac{k_{AB}}{k_{BA}}(1 + K)}$$

which reproduces the result given in eq. (2) of the main text for the typical timescale. The realm of applicability of this expression is not limited to the validity of eq. (1) as also non-markovian transition rates (as would be applicable for small times, see discussion in main text) would ultimately lead to this result. Another approach to the same result, is the reasoning that the effective time should only depend on the probability to be bound which is controlled by the affinity and, thus, would generally lead to a linear term in leading order.

In principle, a very small binding rate k_{on} (or, similarly, a small interaction range) could lead to a crossover in the tail from $\tau(0)$ to $\tau(K)$. However, having a small likelihood for the interaction to take place in the first place would inevitably make it hard to observe. Additionally, this in turn would require a really small unbinding rate, so that the two timescales differ significantly. In summation, we expect eq. (2) of the main text to be an adequate description of the tail behaviour that is actually observed experimentally.

3. Numerical Simulation and Data Evaluation

Our simulations are based on a direct integration of the overdamped Langevin equation (also referred to as Brownian dynamics) to simulate diffusion of particles. This corresponds to an update of particle positions $\boldsymbol{x}_i$ $(i = 1, \ldots, N)$

$$\boldsymbol{x}_i(t + \Delta t) = \boldsymbol{x}_i + \sqrt{2D\Delta t}\boldsymbol{\xi}$$

with $\boldsymbol{\xi}$ a random normal-distributed vector. Interaction is incorporated in a Doi-like fashion, i.e. particles within a threshold radius of R_i have a constant binding rate k_{on}, whereas bound particles have a constant unbinding rate k_{off}. Upon binding the particles switch state and their interparticle distance is constrained to be below R_i, effectively implementing a rather floppy bond. The times for binding and unbinding are evaluated by means of the Gillespie algorithm.

The translation of the positional data $\{\boldsymbol{x}_i\}$ to imaging data $\boldsymbol{y}$ (pixel intensities) is done via convolution with a point-spread function p

$$y_j = \sum_i p(\boldsymbol{x}_i - \boldsymbol{r}_j)$$

with $\boldsymbol{r}_j$ denoting the position (center) of pixel j. In our simulation (consistent with the modeling in tracking software such as the u-track package [4] employed by us) the point-spread function is a Gaussian $p(x) \propto \exp\left(-x^2/(2\sigma^2)\right)$. For diffraction limited imaging, the proper choice would be to use an Airy-Disc whose scale would be completely determined by the imaging (wavelength, numerical aperture). This, however, would ignore the influence of the apparatus (aberrations, . . .), noise from discretization, as well as the influence of exposure time. Both the noise as well as the "motion blur" would lead to additional convolutions with Gaussian filters leading to this effective PSF. The motion blur in principle adds a dependence of the PSF on exposure and therefore on acquisition time. We do not explicitly incorporate this as the effect of motion blur is rather small for typical values. Assuming the underlying "instantaneous" PSF (imaging+apparatus noise) is Gaussian and, also, that the motion on the timescale of the exposure time is Brownian, the effect of the exposure time can be quantified as changing the effective variance σ_0^2 to $\sigma^2 = \sigma_0^2 + \sigma_{\text{exp}}^2$ with $\sigma_{\text{exp}}^2 = Dt_{\text{exposure}}$. Using typical values of $t_{\text{exposure}} = 30\text{ms}$ (in the extremal case of the whole acquisition time being used as exposure time), $D = 0.1(\mu\text{m})^2/\text{s}$, the contribution of exposure is about $\sigma_{\text{exp}}^2 \sim (0.05\mu\text{m})^2$ which is a somewhat negligible contribution to typical PSFs widths of $\sigma^2 \sim (0.3\mu\text{m})^2$ (about 3% of the PSF's area).

We add spatially and temporally uncorrelated noise onto the imaging data to generate our snapshots at fixed intervals $\Delta \gg \Delta t$. This establishes a finite signal-to-noise ratio (SNR). We do, however, not explicitly account for variations in apparent molecule brightness from photon shot-noise, dipole orientation, photo-bleaching, . . . and generally operate at a high SNR. This is

because our focus in this work is the interpretation of detected data. If detection is not accurately feasible, then this is a more fundamental problem and the inference of interaction parameters is not a well posed question anymore. Most of these effects (e.g. photo-bleaching) will introduce their own time-scale on which they become relevant and the order of scales becomes relevant in determining if any inference is still possible.

The simulation is used to generate movies, but also to generate unbiased overlap time distributions. To this end, we keep track of all particle pairs whose distances are below a threshold R_c which are considered to be colocalized. A suitable choice of R_c is a reflection of the detection method used. In particular, the influence of (necessarily) finite detection precision is absorbed into this effective parameter as well as the method's ability to resolve overlapping signals. Using u-track with multi-particle fitting (the program identifies candidate regions and then iteratively determines the number of particles within that region), we found that $R_c \approx 1.5R$ is a good choice. In general, this kind of colocalization decision by means of a thresholding procedure is a step that could be refined in future work.

The movies are then analyzed using u-track (both for detection and tracking). We make use of u-tracks native feature to determine overlaps (starting with a merging event of signals and ended by a splitting event) from trajectories. Alternatively, this could also be done by or with the help of the amplitude information, if one deems that appropriate (no general fluctuations in brightness). We find that this procedure to determine overlaps tends to err on the side of long trajectories. Meaning occasionally a splitting event is not recognized as such which in combination with an erroneous subsequent splitting event later leads to rare very large overlap times. This is the origin of the deviations in the long term tails for all determined overlap time distributions in the main text. We opted not to filter these out, but do not use them for fitting. Fitting for the artificial movies is consistently done in the region where $1 - CDF(t) \in [0.05 : 0.3]$. This ensures that only data points are considered that correspond to at least around 50 trajectories. Fitting is performed by gnuplot throughout.

4. Experimental Details

Experimental data was obtained using H9c2 cell line transfected with Snap-ß$_1$- and Snap-ß$_2$-AR constructs, as previously described [5] for 6 hours to assure suitable expression level for single molecule imaging. They were further labeled with 1μM SNAP-Surface 549 dye (New England Biolabs) for 30 min and washed two times for 10 min. After labeling, the cells were placed in an Oko-Touch Microscope Incubator (Okolab) in FluoroBrite-DMEM (Thermofisher) medium and kept at a temperature of 20°C. The single molecule movies where acquired with a TIRF Eclipse Ti2 microscope (Nikon), using a x100 Apo TIRF objective (1.49 NA), 561-nm laser diode (Nikon) and an iXon Ultra Life 897 EMCCD camera equipped with a Cy3 filter (595/50 nm). Single molecule frames were acquired with an an acquisition time of 30 ms. Perfect-Focus unit (inbuilt, based on near-IR) was used during the time-lapse imaging to retain the focus. This corresponds to a pixel size of approximately 107 nm. The measured PSF waist is 330 nm.

A summary of the relevant quantities is given in the table below.

Acquisition Time	Pixel size	PSF width	measured diffusitivity	pixel timescale	colocalization timescale
Δ [s]	Δ_x [nm]	R [nm]	D [μm^2/s]	$\tau = \Delta_x^2/D$ [s]	$\tau = R^2/D$ [s]
0.03	107	330	≈ 0.05	≈ 0.23	≈ 0.22

References

1. M. E. Fisher, "Walks, walls, wetting, and melting," J. Stat. Phys. **34**, 667–729 (1984).
2. F. D. Stefani, J. P. Hoogenboom, and E. Barkai, "Beyond quantum jumps: Blinking nanoscale light emitters," Phys. today **62**, 34 (2009).

3. S. Winkelmann and C. Schuette, "The spatiotemporal master equation:Approximation of reaction-diffusion dynamics via Markov state modeling," J Chem Phys **145**, 214107 (2016).
4. K. Jaqaman *et al.*, "Robust single-particle tracking in live-cell time-lapse sequences," Nat Methods **5**, 695 (2008).
5. T. Sungkaworn, M.-L. Jobin, K. Burnecki, A. Weron, M. J. Lohse, and D. Calebiro, "Single-molecule imaging reveals receptor–g protein interactions at cell surface hot spots," Nature **550**, 543–547 (2017).